THE EUROPEAN SOCIETY OF MEDICINE
Medical Research Archives, Volume 12 Issue 9

RESEARCH ARTICLE

Effect of Sorbic Acid on the Induction of Static Growth Inhibition in Mouse Mastocytoma P-815 Cells

Yasuyo Okada[1], Yuko Umemoto[1], Hitomi Kimura[1], and Atsushi Ichikawa[1,2*]

[1] School of Pharmacy and Pharmaceutical Sciences, Mukogawa Women's University, 11-68 Kyuban-cho, Koshien, Nishinomiya, Hyogo 663-8179, Japan.
[2] Bio-Education Laboratory, Tawara Building #702, 1-21-33 Higashinakajima, Osaka 533-0033, Japan.

OPEN ACCESS

PUBLISHED
30 September 2024

CITATION
Okada, Y., Umemoto, Y., et al., 2024. Effect of Sorbic Acid on the Induction of Static Growth Inhibition in Mouse Mastocytoma P-815 Cells. Medical Research Archives, [online] 12(9). https://doi.org/10.18103/mra.v12i9.5642

DOI
https://doi.org/10.18103/mra.v12i9.5642

ISSN
2375-1924

ABSTRACT

Sorbic acid and its salts are commonly used as preservatives because of their ability to inhibit the growth of molds, yeasts, and fungi without causing bacterial death. Despite several investigations on sorbic acid-induced static growth inhibition of microorganisms, its implications in mammals remain unexplored. This study investigated the effect of sorbic acid on the growth of mouse mastocytoma P-815 cells (P-815 cells) in culture medium. Our findings indicated that sorbic acid induced static growth inhibition, with optimal results achieved when P-815 cells were exposed to 2.5 mM sorbic acid for at least 48 h, starting approximately 20 h after administration. Notably, the same static growth inhibition by sorbic acid was observed in human promyelocytic leukemia cells but not in mouse bone marrow mast cells. Sorbic acid-induced static growth inhibition increased the number of cells in the G1 and G2 phases and decreased the number of cells in the S phase, demonstrating that sorbic acid affects the cell cycle's G1/S and G2/M transitions. When P-815 cells synchronized at the G1 phase of the cell cycle were treated with sorbic acid, the onset of the cell population was noticeably delayed, whereas S-phase cells revealed almost no delay. The cellular amount of sorbic acid 10 h post-administration was higher in the acidic medium (pH 7.0) than in the medium (pH 7.4), which can be attributed to the inhibition of extracellular release of sorbic acid. Verapamil, a modulator of P-glycoprotein, and sodium azide, an inhibitor of ATP synthesis, inhibited intracellular accumulation of sorbic acid. This suggests that P-glycoprotein plays a role in regulating the intracellular levels of sorbic acid. Administration of sorbic acid led to an increase in intracellular calcium concentration ($[Ca^{2+}]i$), which was suppressed by co-administration with verapamil. Sorbic acid administration decreased the $[Ca^{2+}]i$ levels, which were elevated by thapsigargin, an inhibitor of Ca^{2+}-ATPase in the ER. This inhibitory effect was observed regardless of whether thapsigargin was administered before or after treatment. This is the first study to report that sorbic acid has a static growth inhibitory effect, causing stagnation in the G1 phase in animal cancer cells such as P-815 cells. The primary mechanism involves suppression of thapsigargin-induced intracellular Ca^{2+} release from Ca^{2+} stores in the ER.

Keywords: sorbic acid, static growth inhibition, mastocytoma P-815 cells, cell cycle dependency, intracellular Ca^{2+} concentration

1. Introduction

Sorbic acid (SA) and its salts are commonly used as preservatives. Their antibacterial effects result from the static growth inhibition of molds, yeasts, and fungi [1-10]. The bacteriostatic action of SA is accompanied by metabolic changes in cell membranes, including the inhibition of transport systems and enzymes as well as the creation of a proton flux into cells. One of the main biochemical reactions is intracellular acidification due to the inhibition of H^+-ATPase activity [1-3, 5, 6]. This suggests that SA might affect the pH balance within cells, potentially influencing cell growth and function. However, the precise mechanism by which acidification leads to static growth inhibition of microorganisms remains unclear. While studies using microorganism provide some insight into the potential effects of SA on cells, it is important to note that the response of mammalian cells could be different.

SA is generally recognized as a "Safe Additive" for human consumption. The Joint FAO/WHO Expert Committee on Food Additives suggested an acceptable daily intake (ADI) of 25 mg/kg body weight [11]. This amount is considered safe for individuals to consume daily over their lifetimes without risk. However, the European Food Saftey Authority (EFSA) reports discuss the uncertainties and data gaps related to the effects of SA and recommend further research to better understand these effects [12, 13]. In fact, some studies have indicated SA-induced weak genotoxic potency [14, 15], including DNA damage [16] and the alkyl action of the nucleophilic metabolite 1-(p-nitrobenzyl) pyridine [17]. However, more research is needed to fully understand the effects of SA on the growth suppression of mammalian cells. Notably, no evidence suggesting that SA has a static growth inhibitory effect on mammalian cells has been obtained. In the literature, "static growth inhibition" refers to prolonging the period until cell death, as seen in certain anti-cancer drugs like pyridostatin analogs [18]. In this context, we defined static growth inhibition in mammalian cells as the time required for cell division during cell cycle.

The cell cycle in mammalian cells is a complex process consisting of several phases: the G0 phase (resting state), G1 and G2 phases (involving RNA and protein synthesis), S phase (DNA replication), and M phase (cell division). Unlike normal cells, cancer cells lack the G0 phase and continuously divide [19]. Non-dividing mammalian cell transition from G0 to G1 phase. We investigated the static growth inhibition in cancer cells, focusing on the G1, G2, and S phases. For example, mouse mastocytoma P-815 cells (P-815 cells) exhibit the G1 (2 h), S (4.5 h), G2 (1.5 h), and M (1.5 h) phases during cell cycle synchronization with aphidicolin (Aph) [20]. Considering the constant M phase duration across cell types, fluctuations in the G1, G2, and M phases are crucial for understanding static growth inhibition in cancer cells.

The bacteriostatic activity of SA has been observed to decrease as the pH of the medium becomes more alkaline [3, 6]. In both yeast and *Escherichia coli*, the inhibitory effect induced by SA is attributed to a reaction that alters the intracellular pH ([pH]*i*) [21, 22]. This phenomenon aligns with the classical weak-acid theory, which suggests that undissociated SA permeates the plasma membrane, dissociates within a neutral cytoplasmic pH, releases protons, and inhibits growth by acidifying the cytoplasm. However, this conclusion was challenged because the reaction at [pH]*i* did not directly correlate with decreased cell proliferation [23]. Instead, SA-induced growth inhibition appears to be linked to an increase in the intracellular ADP/ATP ratio owing to elevated ATP consumption in yeast [24]. In mammalian cells, intracellular pH is regulated by various pH-adjustment transporters and channels [25]. Notably, no relationship has been established between [pH]*i* and $[Ca^{2+}]i$ in mammalian cells, although mast cells exhibit ATP-independent luminal oscillations associated with Ca^{2+} and H^+ release from secretory granules [26]. Investigating the interaction between [pH]*i* and $[Ca^{2+}]i$ caused by SA action may provide insight into the signaling mechanisms underlying static growth inhibition in P-815 cells.

The purpose of this study is to suggest that SA, which is primarily understood to have a static growth inhibitory effect on microorganisms, may also have a similar effect on the growth of mammalian cancer cells. Additionally, it aims to suggest that SA may have a new role in the proliferative function of mammalian cancer cells.

2. Materials and methods

2.1. MATERIALS

Fisher's medium was purchased from MP Biomedicals (Irvine, CA, USA) and RPMI 1640 medium was obtained from Sigma-Aldrich (St. Louis, MO, USA). Fetal calf serum (FCS) was obtained from Biowest (Nuaillé, France) and bovine serum albumin (BSA) was obtained from Sigma-Aldrich. EUDRAGIT® L30 D-55 was procured from Evonik Industries AG (Essen, Germany). L-[4,5-^{3}H]leucine, [methyl-^{3}H]thymidine, [5,6-^{3}H]uridine, NCS tissue Solubilizer, and NOCS 104 liquid scintillator were obtained from Amersham Biosciences (Amersham, UK). 5-Bromo-2'-deoxyuridine (BrdU) and nigericin sodium salt were purchased from Sigma-Aldrich, and anti-mouse CD16/CD32 antibody, clone 2.4G2 was procured from Cosmo Bio Co., Ltd. (Tokyo, Japan). 2',7'-Bis-(2-carboxyethyl)-5-(and-6)-carboxyfluorescein, acetoxymethyl ester (BCECF-AM) and propidium iodide (PI) were sourced via DOJINDO (Kumamoto, Japan), and RNase A [EC 3.1.27.5] from bovine pancreas was obtained from Nacalai tesque (Kyoto, Japan). The mouse anti-BrdU-fluorescein isothiocyanate-conjugated monoclonal antibody (FITC-conjugated anti-BrdU mAb) was supplied by Chemicon International, Inc. (Temecula, CA, USA). All other reagents used met guaranteed or liquid chromatography/mass spectrometry (LC/MS) grade standards.

2.2. CELL CULTURE AND VIABILITY TEST

Cell culture methods for P-815 cells [27], human polymyelocytic leukemia cells (HL-60 cells) [28], and mouse bone marrow-derived mast cells (BMMC) [29] have been reported previously. Briefly, P-815 cells were cultured in Fisher's medium supplemented with 10% heat-inactivated FCS. Similarly, HL-60 cells and BMMC were cultured in RPMI 1640 medium, also containing 10% heat-inactivated FCS. All cell cultures were incubated at 37 °C in a CO_2-humidified atmosphere. The viability of the cultured cells was determined using the trypan blue exclusion method. Cell viability was determined using

flow cytometry following the staining of non-viable cells with PI, which was bound to DNA and RNA through intercalation between bases.

2.3. CELL GROWTH

To perform the cell proliferation assay, P-815 cells (1×10^5 cells/mL), HL-60 cells (2×10^5 cells/mL), and BMMC (5×10^5 cells/mL) were cultured in media containing 10% FCS with or without SA at 37 °C for any given time. The total cell number and size were determined using a COULTER Z1 cell counter (Beckman Coulter, Brea, CA, USA).

2.4. ASSAY OF SYNTHESIS OF DNA, RNA, AND PROTEIN

P-815 cells (1×10^5 cells/mL) were seeded into a 6-well tissue culture plate and incubated with or without 2.5 mM SA in an FCS-containing culture medium for 13 h at 37 °C. Thereafter, the cells were subjected to incubation in the presence of 7.4 kBq/mL (1.15 GBq/mmol) [methyl-^{3}H]thymidine, 7.4 kBq/mL (18.26 GBq/mmol) [5,6-^{3}H]uridine, or 18.5 kBq/mL (0.5 GBq/mmol) L-[4,5-^{3}H]leucine for 1 h at 37 °C. Treated cells were collected via centrifugation, washed twice with ice-cold phosphate buffer saline (PBS), homogenized with 5% trichloroacetic acid (TCA), and incubated on ice for 1 h. Acid-insoluble fractions were collected via centrifugation and washed twice with 5% TCA. Subsequently, 5% TCA, NCS Tissue Solubilizer, and NOCS 104 were added to the acid-insoluble fraction. The isotopic content of [^{3}H] in each solubilized acid-insoluble fraction was measured using a liquid scintillation counter LSC-6100 (ALOKA, Tokyo, Japan).

2.5. ANALYSIS OF CELL CYCLE WITH INCORPORATION OF BrdU AND PI STAINING WITH FLOW CYTOMETRY

Ten milliliters of P-815 cells (1×10^5 cells/mL) were seeded into 10 cm tissue culture plates and incubated with or without 2.5 mM SA in an FCS-containing culture medium at 37 °C for any given time. Thereafter the cells were subjected to incubation in the presence of 10 µM BrdU for 1 h at 37 °C. The BrdU-labeled cells were collected via centrifugation, washed twice with ice-cold PBS, then fixed with cold 70% ethanol, followed by washing with 2% FCS/PBS and resuspending in 0.5% Triton X-100/2N HCl for 30 min at 37 °C. After neutralization with 0.1 M $Na_2B_4O_7$, the cell pellets were washed twice with PBS containing 0.5% Tween-20 and 1% FCS, incubated with anti-mouse CD16/CD32 antibody, and clone 2.4G2 in PBS containing 0.5% Tween-20 and 1% FCS on ice for 30 min, and then washed with PBS containing 0.5% Tween-20 and 1% FCS. The washed cell pellets were stained with FITC-conjugated anti-BrdU mAb for 1 h in the dark at room temperature. After washed with PBS containing 2% FCS, they were incubated with PI (0.1 mg/mL) and RNAse A (10 µg/mL) for 5 min at room temperature. The samples were analyzed using a FACScan flow cytometer (Nippon Becton Dickinson, Tokyo, Japan) and CellQuest Pro software (Nippon Becton Dickinson).

2.6. PREPARATION OF SYNCHRONOUS CELLS

P-815 cells (1×10^5 cells/mL) were synchronized for growth by exposure of 100 µM epigallocatechin gallate (EGCG) for 15 h [30] for adjusting the cell cycle in the G1 phase, and by exposure of 1 mM Aph for 15 h [20] in the S phase.

2.7. QUANTITATIVE ANALYSIS OF AMOUNT OF SORBIC ACID UPTAKE IN P-815 CELLS

Ten milliliters of P-815 cells (1×10^5 cells/mL) were seeded into 10 cm tissue culture plates and incubated with 2.5 mM SA in an FCS-containing culture medium at 37 °C for any given time. After stopping the reaction, the cells were collected via centrifugation at 2,300 × *g* for 5 min at 4 °C and washed twice with cold PBS. The washed cells were sonicated in PBS using a SONIFIER (BRANSON, Kanagawa, Japan) and filtered using a Nanosep 10 K device (Pall Life Sciences, Port Washington, NY, USA) to measure the amount of SA via LC/MS/MS analysis, which we previously developed [31] (Section 2.8).

2.8. LC/MS/MS ANALYSIS

The LC/MS/MS analysis was performed using a Quattro Premier triple-quadrupole LC/MS system (Micromass, Manchester, USA) equipped with an ESI source (negative ionization mode) coupled to an HT Waters 2795 separation module (Waters Co. Milford, MA, USA). The mass spectrometer was operated at low resolution for both Q1([M-H]$^-$ m/z 111) and Q3 (m/z 67) in SRM mode. Data were acquired using the MassLynx software (Waters). Chromatographic separation of SA using TSKgel ODS100V (4.6 mm i.d. × 150 mm) from TOSOH Co. (Tokyo, Japan) was performed at a flow rate of 0.4 mL/min, acetonitrile-water (40:60) as the mobile phase.

2.9. MEASUREMENT OF [PH]*I* WITH FLUORESCENT PH INDICATOR BCECF-AM

P-815 cells were washed with 0.1% BSA in 153 mM NaCl, 5 mM KCl, 5 mM glucose, and 20 mM HEPES (pH 7.4) (HBS buffer) and adjusted at a density of 4×10^7 cells/mL, following incubation with 3 µM BCECF-AM for 30 min in the dark at 37 °C. The cells were washed twice with HBS buffer and the cell density was adjusted to 1×10^6 cells/mL. The cell suspension was placed in a cuvette and treated with 1, 2.5, or 5 mM SA as the stimulating agent. Calibration of the [pH]*i* was performed using the nigericin/K^+ method [32]. The fluorescence intensities were measured at excitation and emission wavelengths of 450, 500, and 540 nm using a fluorescence spectrometer CAF-110 (Jasco, Tokyo, Japan).

2.10. MEASUREMENT OF INTRACELLULAR FREE Ca^{2+} USING Fura-2 AM

Cytosolic Ca^{2+} concentration was measured using Fura-2 AM, as previously described [33]. Fluorescence intensities were measured at excitation and emission wavelengths of 340, 380, and 510 nm using a fluorescence spectrometer (CAF-110).

2.11. STATISTICAL ANALYSIS

Data are shown as the mean ± standard deviation (SD) of three or more experiments. Comparisons between the two groups were made using the Student's *t* test. To compare more than two groups with comparable variances, one-way ANOVA was first performed, and Dunnett's test was then used to evaluate pairwise group differences. Values of $*P < 0.05$, $**P < 0.01$, and $***P < 0.005$ were considered statistically significant.

3. Results

3.1. ADMINISTRATION OF SORBIC ACID TO P-815 CELLS RESULTS IN STATIC GROWTH INHIBITION WITHOUT CAUSING CYTOTOXICITY

Administration of 2.5 mM SA significantly suppressed P-815 cell growth. This effect began approximately 10 h after administration and persisted for 48 h (Fig. 1 (A)-1). Growth inhibition occurred in a concentration-dependent manner, leading to the selection of 2.5 mM for subsequent experiments. As shown in Figure 1 (A)-1, SA-treated cells had a doubling time of approximately 15 h, whereas target cells exhibited a doubling time of approximately 12 h. In addition, SA inhibited the growth of cancerous HL-60 cells and P-815 cells but not that of non-cancerous BMMC (Fig. 1 (A)-2 and -3). No significant increase in cell death was observed in SA-treated P-815 cells over at least three days of culture using the trypan blue staining method (data not shown). By reference to the report that the bacteriostatic effect of SA was high in acidic medium [9], P-815 cells were cultured in medium at pH 7.0 adjusted using Eudragit® a pH-sensitive polymer (Fig. 1 (B)). The inhibitory effect of SA was twice as strong in a pH 7.0 culture medium compared to that at pH 7.4. These findings suggest that SA has potential as an anticancer agent, particularly in acidic environments. In cultured cells, essential macromolecules, such as DNA, RNA, and proteins, are continuously synthesized *de novo*. In cultured cell experiments using radioisotopes, when P-815 cells were treated with SA for 13 h, the synthesis of radiolabeled precursor nucleotides and amino acids by macromolecules was inhibited by approximately 40% (Fig. 1 (C)). This inhibition highlights the effects of SA on cellular processes and its potential as a modulator of biological pathways.

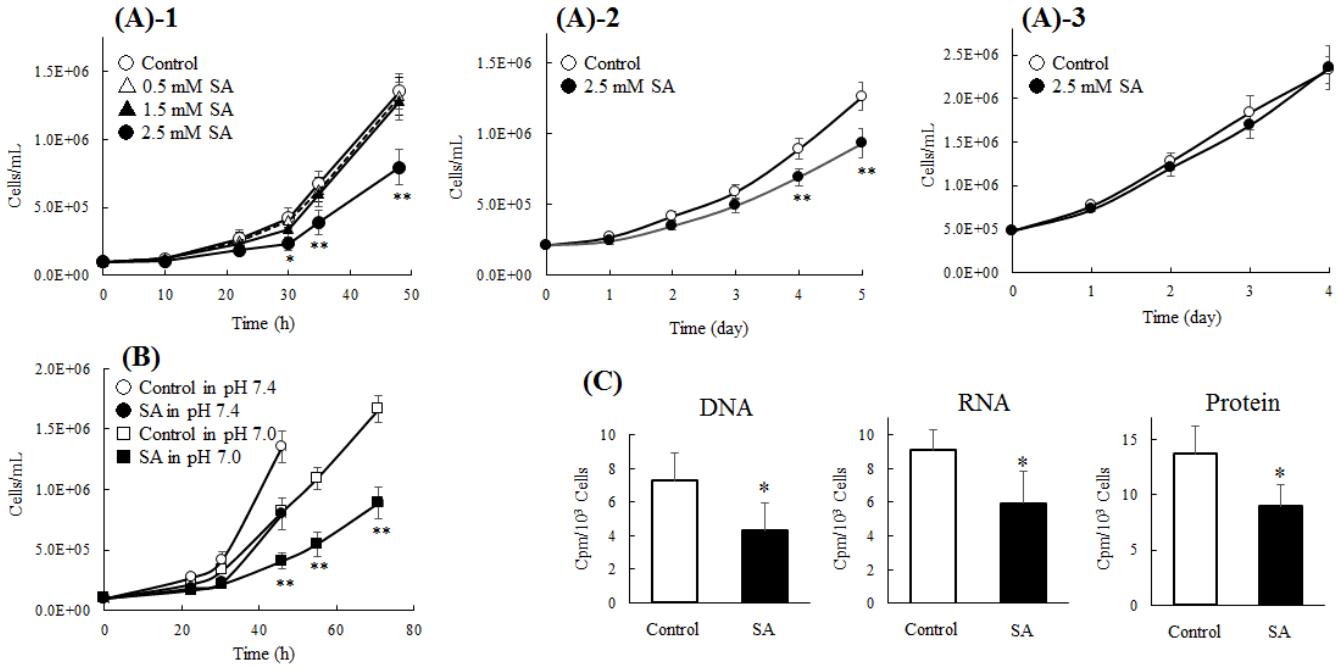

Fig. 1. Effects of SA on cell proliferation rate and synthesis of DNA, RNA, and protein.

(A) Effects of SA on the proliferation of P-815 cells, HL-60 cells, and BMMC.

P-815 cells (1 × 10^5 cells/mL, (A)-1), HL-60 cells (2 × 10^5 cells/mL, (A)-2), and BMMC (5 × 10^5 cells/mL, (A)-3) were cultured over time treatment with or without SA. $^{**}P < 0.01$; $^{*}P < 0.05$: SA-treated cells versus SA-untreated cells.

(B) Effects of SA in acidic media.

P-815 cells (1 × 10^5 cells/mL) were cultured in either a general medium (pH 7.4) or acidic medium (pH 7.0) adjusted with EUDRAGIT® L30 D-55. Proliferation rate was measured over time after treatment with or without 2.5 mM SA. $^{**}P < 0.01$: SA-treated P-815 cells in pH 7.0 versus SA-untreated P-815 cells in pH 7.0.

(C) Effect of SA on biomolecule synthesis.

P-815 cells (1 × 10^5 cells/mL) were cultured and treated with or without 2.5 mM SA. The synthesis levels of DNA, RNA, and proteins were measured as described in Section 2.4. $^{*}p < 0.05$: SA-treated P-815 cells versus SA-untreated P-815 cells.

3.2. ADMINISTRATION OF SORBIC ACID LEADS TO A REDUCTION IN THE CELL SIZE OF P-815 CELLS AND ARRESTS MOST OF THESE CELLS IN THE G1 PHASE OF THE CELL CYCLE

The results of the cell counter assay revealed that administration of SA for 10 and 23 h significantly reduced the size of most P-815 cells. Notably, after 44 h, the size of the SA-treated P-815 cells returned to normal (Fig. 2). Smaller cells are typically in the G1 phase of the cell cycle [30]. Therefore, most of the SA-treated P-815 cells remained in the G1 phase during the 10–23 h period following SA administration.

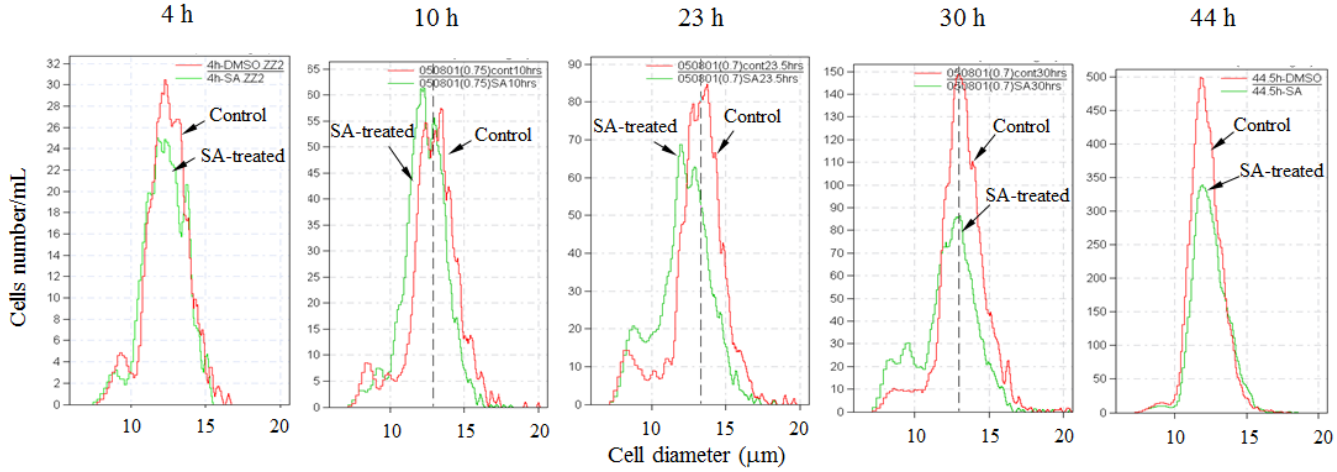

Fig. 2. Effect of SA on cell size of P-815 cells.
P-815 cells (1 × 10^5 cells/mL) were treated with (green line) or without (red line) 2.5 mM SA, and cell size, expressed as cell diameter, was measured over time. Similar results were obtained in three or more experiments and a representative example is presented.

The impact of SA administration on the cell cycle phases in P-815 cells was investigated using flow cytometry analysis of cells stained with FITC-conjugated anti-BrdU mAb and PI (Fig. 3 (A)). Based on this result, the percentage of the G1, S, and G2/M phase-localized P-815 cells were determined over time (Fig. 3 (B)). SA-treated P-815 cells revealed an increased proportion of cells in the G1 phase. SA-treated P-815 cells also exhibited an increased proportion of cells in the G2/M phase. Conversely, the proportion of S-phase P-815 cells decreased from 6–20 h after SA administration. After 20 h post-SA administration, there was no significant difference in the cell cycle between SA-treated and untreated cells.

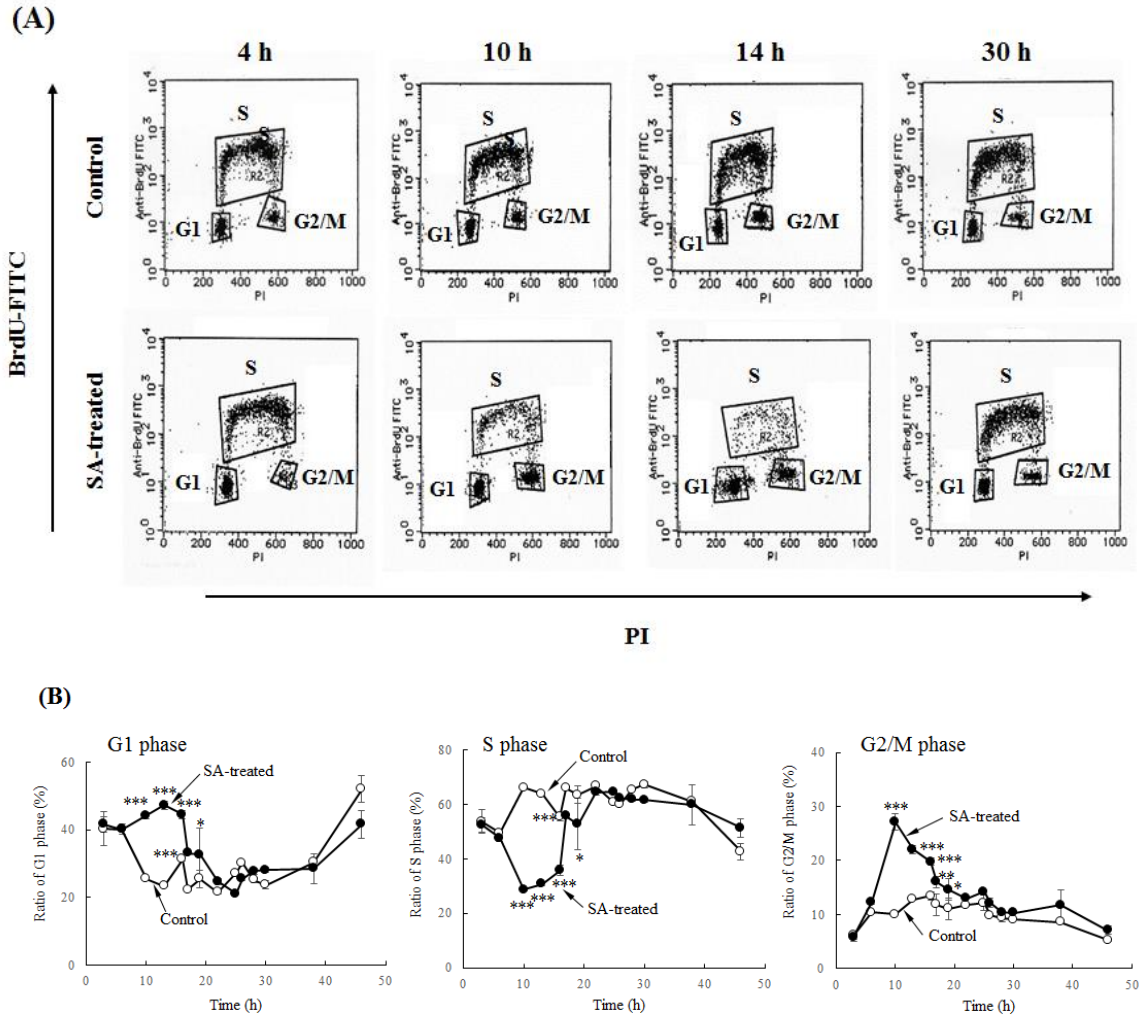

Fig. 3. Effect of SA on cell cycle progression in P-815 cells.
P-815 cells (1 × 10^5 cells/mL) incubated with or without 2.5 mM SA in the medium were stained with BrdU and PI, as described in Section 2.5, and subsequently analyzed via FACS. (A) Representative histograms of the cell cycle in P-815 cells treated with or without SA. (B) Effect of SA on the proportion of each phase of the cell cycle in P-815 cells. ***$p < 0.005$; **$p < 0.01$; *$p < 0.05$: SA-treated P-815 cells versus SA-untreated P-815 cells.

Further investigation revealed that P-815 cells were synchronized in different phases of the cell cycle: the G1 phase using EGCG and the S phase using Aph. In P-815 cells arrested in the G1 phase, the start time of proliferation of SA-treated P-815 cells was approximately five times slower than that of untreated P-815 cells (Fig. 4 (A)). In contrast, in the S phase of the cell cycle, the start time of proliferation of SA-treated P-815 cells was not significantly different from that without SA administration. The early onset of proliferation in S phase-synchronized P-815 cells with or without SA administration was faster than that in unsynchronized P-815 cells (Fig. 4 (B)). This rapid increase in the number of dividing cells may be due to the simultaneous initiation of cell proliferation in synchronous cells. Notably, similar results were obtained using other synchronized culture reagents such as dexamethasone for G1-arrested P-815 cells and hydroxyurea for S-phase-arrested P-815 cells (data not shown).

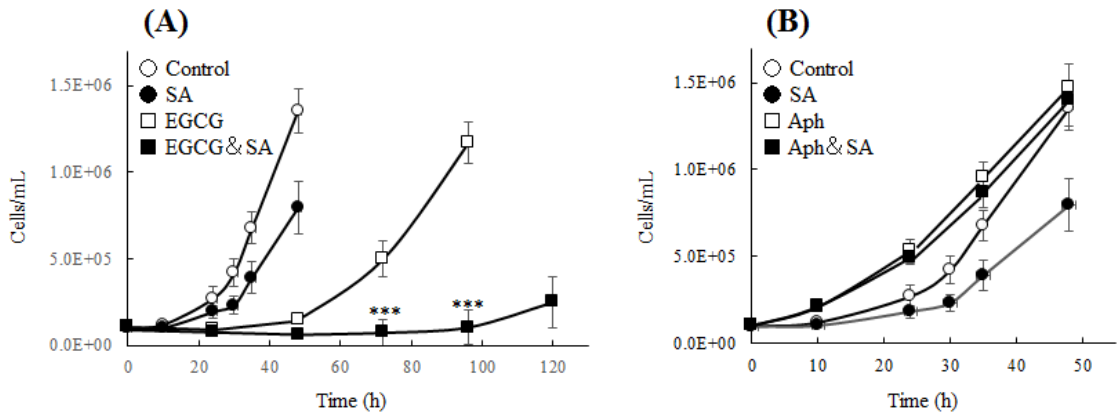

Fig. 4. Effect of SA on cell proliferation rate of P-815 cells arrested in the G1 phase or S phase of the cell cycle. P-815 cells were arrested in the G1 phase with EGCG (A) or in the S phase with Aph (B) of the cell cycle, as described in Section 2.6. P-815 cells (1×10^5 cells/mL) were cultured and the cell proliferation rate was measured over time following treatment with or without 2.5 mM SA. ***$p < 0.005$: SA and EGCG-treated P-815 cells versus EGCG-treated P-815 cells

3.3. CHANGES IN THE INTRACELLULAR AMOUNT OF SORBIC ACID IN P-815 CELLS

3.3.1 Effect of the pH 7.4- or pH 7.0-culture medium

As shown in Figure 1(B), the inhibition of cell proliferation by SA was stronger in an acidic medium pH 7.0 than in a neutral medium (pH 7.4). This study investigated whether the pH of the medium affects the amount of SA uptake by cells. Thus, the aim was to determine whether the difference in the inhibitory effect was due to variations in intracellular SA uptake. Using LC/MS/MS [31], we examined the intracellular amount of SA after its administration in P-815 cells incubated in either control medium (pH 7.4) or acidic medium (pH 7.0). P-815 cells incubated in either culture medium immediately took up SA, which peaked at 5 h. These levels were maintained for an additional 10 h before they gradually decreased. At 24 h post-SA administration, SA levels were approximately one-fourth of the plateau level for P-815 cells in the culture medium at pH 7.4, and approximately half of the plateau level for P-815 cells in pH 7.0 culture medium (Fig. 5). That is, the rate of SA reduction incubated for 13–24 h post-administration was slower in cells housed in a pH 7.0 culture medium compared with those in the medium at pH 7.4. This suggests that the release of intracellular SA may have been suppressed. This intracellular accumulation of SA occurred before the onset of the inhibitory effect on cell proliferation, starting 20–30 h after post-SA administration (Fig. 1(B)). This result is similar to the growth inhibition mechanism observed under acidic conditions in yeast and *E. coli* cells [21, 22].

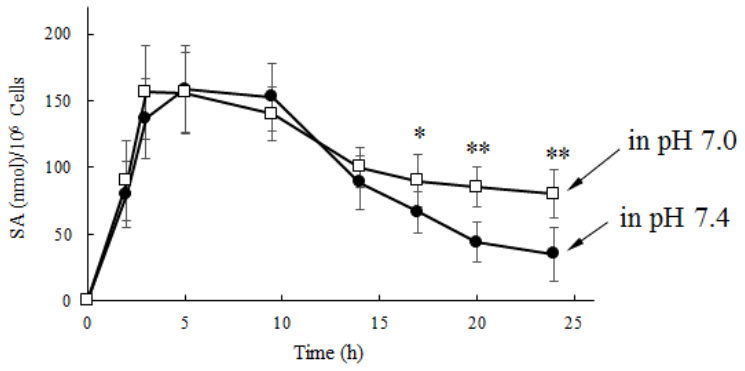

Fig. 5. Changes in SA uptake in P-815 cells incubated in the pH 7.4- or pH 7.0-culture medium. P-815 cells (1×10^5 cells/mL) were cultured over time with 2.5 mM SA in general medium (pH 7.4) or acidic medium (pH 7.0) adjusted with EUDRAGIT® L30 D-55. Cellular SA levels were measured as described in Sections 2.7 and 2.8. **$p < 0.01$; *$p < 0.05$: SA-treated P-815 cells in pH 7.0 medium versus SA-treated P-815 cells in pH 7.4 medium.

3.3.2. Changes in sorbic acid uptake in P-815 cells pretreated with either verapamil or sodium azide

The experimental results in Figure 5 show that the intracellular accumulation of SA was due to decreased extracellular release of SA. P-glycoprotein is an important efflux pump responsible for the extrusion of many endogenous and exogenous substances from cells [34]. We previously confirmed that P-815 cells express P-glycoprotein at the protein level using western blotting [27] and that verapamil is known to dose-dependently inhibit the antigen-induced release of mediators from mast cells because of its calcium antagonistic effect [35]. Therefore, we investigated whether verapamil, a modulator of the P-glycoprotein belonging to the ATP-binding cassette, affected the intracellular accumulation of the administered SA. As shown in Figure 6, pre-administration of either verapamil or sodium azide for 0.5 h significantly reduced the post-uptake of SA, as measured at 8 h post-administration. This is the first study showing that SA uptake in P-815 cells involves pathways affected by verapamil administration.

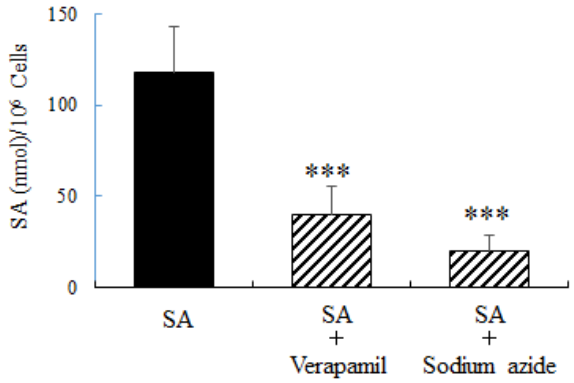

Fig. 6. Effects of verapamil or sodium azide on intracellular uptake of SA in P-815 cells.

P-815 cells (1 × 10^5 cells/mL) were incubated in medium containing 10% FCS with or without 100 μM verapamil or 2.0 mM sodium azide at 37 °C for 30 min, followed by the addition of 2.5 mM SA for 8 h. A quantitative analysis of the intracellular uptake of SA was performed as described in Sections 2.7 and 2.8. ***$p < 0.005$: P-815 cells treated with SA versus P-815 cells treated with SA and verapamil or sodium azide.

3.4. EFFECT OF SORBIC ACID ON CHANGES IN [PH]*i* OF P-815 CELLS

Previous studies have shown that sorbic acid, when administered in the medium, decreases [pH]*i* in cells of *E. coli* [36] due to intracellular acidification, which results from the inhibition of H^+-ATPase activity [1-3, 5, 6]. Therefore, we examined whether SA administration lowered [pH]*i* in P-815 cells. Figure 7 shows a typical example of [pH]*i* changes after the administration of different concentrations of SA (1–5 mM), which were measured using the fluorescent pH indicator BCECF-AM. [pH]*i* quickly shifts to a lower value depending on the concentration of SA administered. When expressed as the values of at least three experiments SA-treated P-815 cells for 20 min after SA administration, [pH]*i* in the vehicle cells was 7.47–7.54, which was shifted to 7.39–7.46 in 1 mM SA-treated cells, 7.29–7.37 in 2.5 mM SA-treated cells, and 7.01–7.20 in 5 mM SA-treated cells. This result shows that as the concentration of SA increased, the proportion of the molecular form of SA increased, which dissociated into hydrogen ions in the cytoplasm, resulting in a low value of [pH]*i*.

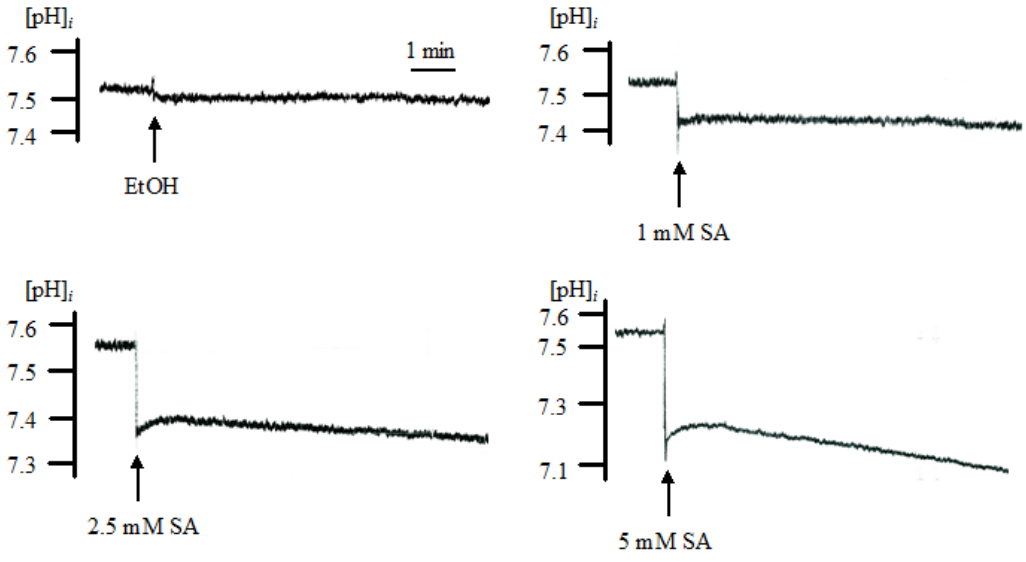

Fig. 7. Effect of SA on [pH]*i* in P-815 cells.

P-815 cells (4 × 10^7 cells/mL) were treated with the fluorescent pH indicator BCECF-AM and then incubated with or without 2.5 mM SA, and [pH]*i* was assayed using the nigericin/K^+ method, as described in Section 2.9.

3.5. Ca^{2+} MOBILIZATION IN P-815 CELLS WITH A SINGLE ADMINISTRATION OF EACH OF SORBIC ACID OR THAPSIGARGIN, OR A COMBINED ADMINISTRATION OF TWO OF THEM

Several studies have investigated the interactions between [pH]*i* and [Ca^{2+}]*i* in cultured cells, including mast cells [37]. We then investigated the changes in [Ca^{2+}]*i* mobilization using the Ca^{2+}-sensitive fluorescent ratiometric dye Fura-2 AM. SA administration caused a reaction that increased rapidly and quickly reached a plateau in the Ca^{2+} ratio with an increase in [Ca^{2+}]*i* (Fig. 8 (A)). In contrast, the Ca^{2+} ratio caused by the administration of the Ca^{2+}-ATPase inhibitor, thapsigargin, increased immediately and strongly (Fig. 8 (B)). The increase in thapsigargin treatment was suppressed by prior (Fig. 8 (C)) and post-administration of SA (Fig. 8 (D)). In contrast, the administration of verapamil (2.5 mM) did not affect the Ca^{2+} ratio (Fig. 9 (A)), and notably, the change in the Ca^{2+} ratio following the post-administration of SA disappeared (Fig. 9 (B)). This suggests that SA uptake is regulated through a verapamil-sensitive P-glycoprotein pathway.

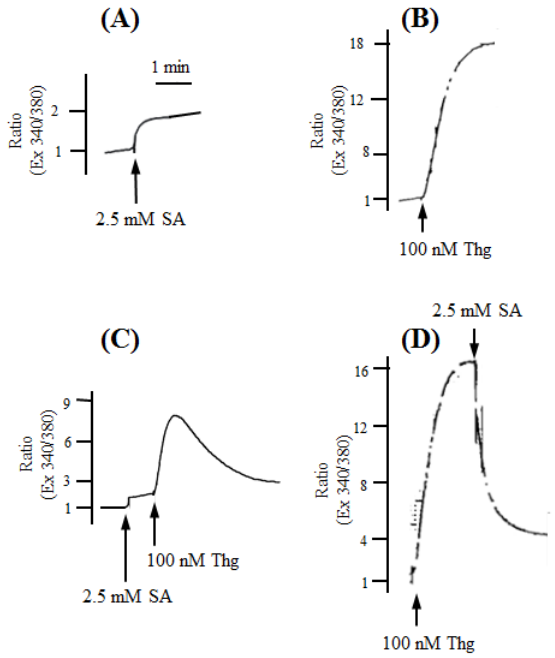

Fig. 8. Ca^{2+} mobilization in P-815 cells treated with SA and/or thapsigargin.
P-815 cells (1 × 10^6 cells/mL) were treated with either 2.5 mM SA (A) or 100 nM thapsigargin (Thg) (B), and subsequently with 2.5 mM SA followed by 100 nM Thg (C) and 100 nM Thg followed by 2.5 mM SA (D), sequentially. Arrows indicate the time points of drug administration. [Ca^{2+}]*i* was measured as changes in the fluorescence intensity of 2 μM Fura-2 AM.

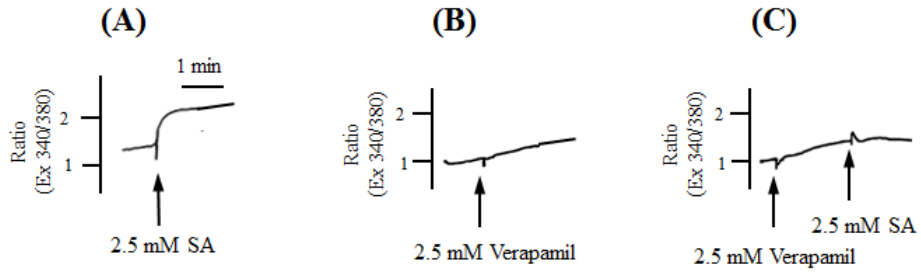

Fig. 9. Ca^{2+} mobilization in P-815 cells treated with verapamil and/or SA.
P-815 cells (1 × 10^6 cells/mL) were treated with either 2.5 mM SA (A) or 2.5 mM verapamil (B), and subsequently with 2.5 mM verapamil followed by 2.5 mM SA (C) The time points of drug administration are indicated by the arrows. [Ca^{2+}]*i* was measured by changes in the fluorescence intensity of 2 μM Fura-2 AM.

4. Discussion

SA is a weak acid used as a preservative in foods, pharmaceuticals, and cosmetics. When microorganisms, including *Saccharomyces cerevisiae* and *E. coli*, are exposed to weak acids such as SA, their growth is inhibited without being killed [1-3, 5, 6, 21, 22]. This inhibition occurred because of intracellular acidification and anion accumulation. Microorganisms survive and multiply in the presence of weak acids. Although various mechanisms contribute to the inhibition of static growth, a comprehensive and quantitative understanding remains elusive [23]. The lack of direct evidence regarding static growth inhibition by SA in mammalian cells is intriguing, particularly considering its widespread use as a preservative. One possible reason for this is the absence of suitable cells for the investigation. Unlike typical

mammalian cells, which follow a cycle of growth, division, and eventual death, cancer cells deviate from this pattern and multiply uncontrollably, leading to tumor formation. Notably, cancer cells and microorganisms lack the G0 phase of their cell cycle. In the present study, we observed that SA administration induced static growth inhibition in P-815 cells cancer cells without causing cell death. Notably, a similar effect was observed in HL-60 cancer cells but not in normal BMMC. Although this evidence is not conclusive, it supports the theory that SA inhibits the static growth of cancer cells. Furthermore, the fact that cell death did not occur in P-815 cells even after prolonged exposure to SA for at least three days, suggests that static growth inhibition occurred.

The effect of SA on the cell cycle occurs during the G1/S and G2/M transition periods. When SA was administered, the proportion of cells in the G1 and G2 phases increased, and that in the S phase decreased. Notably, the decrease in the number of cells in the S phase (Fig. 3 (B)) corresponds to a reduction in DNA synthesis (Fig. 1 (C)). However, SA administration also increased the number of cells in the G1 phase (Fig. 3 (B)), despite a decrease in RNA and protein synthesis (Fig. 1 (C)). This apparent contradiction suggests that a specific reaction may be responsible for the static growth inhibitory effect of SA, possibly due to a reduction in RNA and protein synthesis.

In microorganisms, static growth inhibition by SA occurs due to the creation of an acidic environment inside the cell. This is caused by SA-induced inhibition of H^+-ATPase, an enzyme responsible for proton efflux, via an exchange reaction involving K^+/protons coupled with ATP hydrolysis [1-3]. In *S. cerevisiae*, both H^+-ATPase and glycolytic flux are essential for growth adaptation in the presence of SA as a preservative [3, 10, 38]. Stratford et al. reported that the administration of growth-inhibitory concentrations of SA reduced the intracellular pH in *S. cerevisiae* to 6.3 [9]. Interestingly, in the case of P-815 cells, $[pH]i$ decrease induced by 2.5 mM SA was only from 7.39–7.46 to 7.29–7.37 (Fig. 7 and Result 3.4). The acidification of $[pH]i$ depends on the amount of molecular form that is incorporated. We calculated the amount of molecular SA necessary to achieve a specific value in P-815 cells incubated in medium at pH 7.0 and pH 7.4. According to the traditional Henderson-Hasselbalch equation [39], the proportion of the molecular form of SA is approximately 0.23% of 2.5 mM SA in a medium at pH 7.4, and 0.57% in a medium at pH 7.0. The percentage of the molecular forms of SA in a medium at pH 7.0 is 2.5 times greater than that in a medium at pH 7.4. This higher amount of molecular SA results in a decrease in $[pH]i$ (Fig. 5), which is associated with the mechanism that causes retardation in the proliferation rate of P-815 cells in the medium at pH 7.0 compared to that at pH 7.4 (Fig. 1(B)). The regulation of $[pH]i$ in membrane enzymes and glycolysis of yeast mutants [40], as well as mast cell functions [41-43], is reported to involve several mechanisms. These include Na^+-H^+ exchange, CO_3H^- influx, Na^+-Ca^{2+} exchange, Na^+-K^+-ATPase, and Ca^{2+}-pH crosstalk. However, few studies have explored the signals linking $[pH]i$ changes to cell proliferation. We focused on $[Ca^{2+}]i$ as a signal related to $[pH]i$ changes because mast cells exhibit ATP-independent luminal oscillations associated with Ca^{2+} and H^+ release from secretory granules [26]. Additionally, the presence of CO_3H^- limits recovery from acute intracellular acidification, likely via the Na^+-independent $Cl^-CO_3H^-$ exchanger, modulates the regulation of $[pH]i$ by protein kinase C and calcium signaling pathways [44].

Verapamil, a P-glycoprotein modulator, is recognized as a blocker of smooth muscle cell Ca^{2+} channel [45]. Verapamil inhibits dose-dependent antigen-induced degranulation of mast cells because of its calcium antagonistic effect [35]. Experiments involving SA uptake in P-815 cells have shown that verapamil decreased the intracellular accumulation of SA (Fig. 6)) and counteracted the SA-induced increase in the Ca^{2+} ratio (Fig. 9). This suggests that SA uptake or removal from P-815 cells may be mediated by verapamil-sensitive P-glycoprotein. On the other hand, further SA taken into cells regulates $[Ca^{2+}]i$ in thapsigargin-induced P-815 cells. Administration of SA rapidly induced an increase in $[Ca^{2+}]i$ caused by thapsigargin. Considering that $[Ca^{2+}]i$ is essential for cell proliferation, metabolism, and gene transcription, the inhibitory effect of SA on thapsigargin-induced $[Ca^{2+}]i$ may contribute to the static growth inhibition observed in P-815 cells.

An important effect of SA revealed in this experiment was the increase in G1 cells in the cell cycle of P-815 cells, and we considered the relationship between these events and thapsigargin-induced $[Ca^{2+}]i$ changes. SA administration arrested the cell cycle of P-815 cells at the G1 phase (Fig. 3), and the start time of proliferation of SA-treated P-815 cells, previously arrested in the G1 phase, was approximately five times slower than that of SA-untreated P-815 cells (Fig. 4). These changes depend on alterations in the concentration of $[Ca^{2+}]i$, as changes in $[Ca^{2+}]i$ correlate with specific events such as elongation of the G1 phase and hindered progression through the G1/S transition in HEK 293 cells [46]. Additionally, the G1/S phase transition is triggered by an increase in $[Ca^{2+}]i$ in rodent vascular smooth muscle cells [47]. Furthermore, $[Ca^{2+}]i$ fluctuations are finely regulated by the concerted interaction of membrane receptors and ion channels that introduce Ca^{2+} into the cytosol, as well as by Ca^{2+}-clearing mechanisms that restore Ca^{2+} to pre-stimulation levels and prevent cytotoxic Ca^{2+} overload [48]. Although the point of action of SA requires further investigation, it may control the stimulus-response reaction that regulates $[Ca^{2+}]i$, which may be necessary for the initiation and maintenance of the G1 phase.

The G1/S transition is a critical stage in the cell cycle, making the boundary between the G1 phase, where the cell grows, and the S phase, where DNA is replicated. Here are some key events that occurs at this transition: (1) Cell cycle checkpoints to ensure cellcycle integrity. (2) Cellular decisions to makes decisions to become quiscient (enter G0), differentiate, make DNA repairs, or proliferate based on environmental cues and molecular signaling input. (3) Regulation by the transcription factor p53, and cyclin D-Cdk4/6 dimer, which phosphorylates the retinoblastoma protein, releasing the transcription factor E2F. (4) Often reffered to as a “point of no return”. Once a cell passes through this transition, it will continue through the cell cycle regardless of incoming mitogenic factors. Thus, the G1/S border, where G1 phase cells transition to S phase cells, involves various reactions and

control systems. It is a major challenge for future research to determine which of these reactions are influenced by SA, and how it contributes to the generation and maintenance of static growth inhibitory cells.

5. Conclusion

Collectively, these findings demonstrate that SA induces static growth inhibition by arresting cell cycle transitions from G1 to S and G2 to M phases in P-815 cells. Additionally, SA plays an essential role in the downregulation of $[Ca^{2+}]i$ required for the initiation and maintenance of G1 progression during cell cycle progression. Unlike cancer cells, the transition from the G1 to S phase in normal cells is not clearly understood. This may explain the difficulty of recognizing the effects of SA. Further research on the effect of SA on the activity of Ca^{2+}-ATPase in G1/S transition is required to address this issue.

Conflicts of interest: The authors have no conflicts of interest to declare.

Author's contributions: A.I. designed the study, analyzed the data, and edited the manuscript; Y.O. conceived and designed the study, performed the cellular experiments, analyzed the data, wrote and prepared the manuscript, and edited the manuscript; Y.U. and H.K. performed the cellular experiments, analyzed the data, and edited the manuscript.

Acknowledgments: We would like to thank Editage (www.editage.jp) for the English language editing.

Funding Statement: None.

References

1. Plumridge A, Hesse SJ, Watson AJ, Lowe KC, Stratford M, Archer DB. The weak acid preservative sorbic acid inhibits conidial germination and mycelial growth of *Aspergillus niger* through intracellular acidification. *Appl Environ Microbiol*. 2004;70(6):3506–11. doi:10.1128/AEM.70.6.3506-3511.2004.
2. Bracey D, Holyoak CD, Coote PJ. Comparison of the inhibitory effect of sorbic acid and amphotericin B on *Saccharomyces cerevisiae*: is growth inhibition dependent on reduced intracellular pH?. *J Appl Microbiol*. 1998;85(6):1056–66. doi:10.1111/j.1365-2672.
3. Holyoak CD, Stratford M, McMullin Z, Cole MB, Crimmins K, Brown AJ, Coote PJ. Activity of the plasma membrane H^+-ATPase and optimal glycolytic flux are required for rapid adaptation and growth of *Saccharomyces cerevisiae* in the presence of the weak-acid preservative sorbic acid. *Appl Environ Microbiol*. 1996;62(9):3158-64. doi:10.1128/aem.62.9.3158-3164.1996.
4. Sofos JN, Busta FF, Allen CE. Sodium nitrite and sorbic acid effects on *Clostridium botulinum* spore germination and total microbial growth in chicken frankfurter emulsions during temperature abuse. *Appl Environ Microbiol*. 1979;37(6):1103-9. doi:10.1128/aem.37.6.
5. Ronning IE, Frank HA. Growth inhibition of putrefactive anaerobe 3679 caused by stringent-type response induced by protonophoric activity of sorbic acid. *Appl Environ Microbiol*. 1987;53(5):1020-7. doi:10.1128/aem.53.5.1020-1027.1987.
6. Sun R, Vermeulen A, Devlieghere F. Modeling the combined effect of temperature, pH, acetic and lactic acid concentrations on the growth/no growth interface of acid-tolerant *Bacillus* spores. *Int J Food Microbiol*. 2021; 360:109419. doi: 10.1016/j.ijfoodmicro.
7. Wang Q, Peng Y, Chai L, Ding W. Antimicrobial effect of sorbic acid-loaded chitosan/ tripolyphosphate nanoparticles on *Pseudomonas aeruginosa*. *Int J Biol Macromol*. 2023; 226:1031-40. doi:10.1016/j.ijbiomac:2022.11.220.
8. Stratford M, Vallières C, Geoghegan IA, Archer DB, Avery SV. The preservative sorbic acid targets respiration, explaining the resistance of fermentative spoilage Yeast species. *mSphere*. 2020;5(3):e00273-20. doi: 10.1128/mSphere.00273-20.
9. Stratford M, Nebe-von-Caron G, Steels H, Novodvorska M, Ueckert J, Archer DB. Weak-acid preservatives: pH and proton movements in the yeast *Saccharomyces cerevisiae*. *Int J Food Microbiol*. 2013;161(3):164-71. doi:10.1016/j.ijfoodmicro.2012.12.013.
10. Ullah A, Chandrasekaran G, Brul S, Smits GJ. Yeast adaptation to weak acids prevents futile energy expenditure. *Front Microbiol*. 2013;4:142. doi: 10.3389/fmicb.2013.00142.
11. Younes M, Aquilina G, Castle L, Engel KH, Fowler P, Jose M, Fernandez F, Fürst P, Gürtler R, Gundert-Remy U, Husøy T, Mennes W, Moldeus P, Oskarsson A, Shah R, Wölfle D, Lambré C, Christodoulidou A, Waalkens-Berendsen I. Opinion on the follow-up of the re-evaluation of sorbic acid (E200) and potassium sorbate (E202) as food additives. *EFSA J*. 2019;17(3):e05625. doi:10.2903/j.efsa.2019.5625.
12. Nemes D, Kovács R, Nagy F, Tóth Z, Herczegh P, Borbás A, Kelemen V, Pfliegler WP, Rebenku I, Hajdu PB, Fehér P, Ujhelyi Z, Fenyvesi F, Váradi J, Vecsernyés M, Bácskay Il. Comparative biocompatibility and antimictobial studies of sorbic acid derivatives. *Eur J Pharm Sci*. 2020;143:105162. doi:10.1016/j.ejps.2019.105162.
13. Aguilar F, Crebelli R, Domenico AD, Dusemund B, Frutos MJ, Galtier P, Gott D, Gundert-Remy U, Lambré C, Leblanc JC, Lindtner O, Moldeus P, Mortensen A, Mosesso P, Parent-Massin D, Oskarsson A, Stankovic I, Waalkens-Berendsen I, Woutersen RA, Wright M, Younes M. Scientific opinion on the re-evaluation of sorbic acid (E200), potassium sorbate (E202) and calcium sorbate (E203) as food additives. *EFSA J*. 2015;13(6):4144, 28pp. doi:10.2903/j.efsa.2015.4144.
14. Winkler C, Frick B, Schroecksnadel K, Schennach H, Fuchs D. Food preservatives such as sodium sulfite and sorbic acid suppress mitogen-stimulated peripheral blood mononuclear cells. *Food Chem Toxicol*. 2006;44(12):2003-7. doi:10.1016/j.fct.2006.06.019.
15. Munzer R, Guigas C, Renner HW. Re-examination of potassium and sodium sorbates for their possible genotoxic potential. *Food Chem Toxicol*. 1990;28(6):397-401. doi:10.1016/0278-6915(90)90085-2.
16. Ferrand C, Mark F, Cassand P, Saint Blanqut G. Mutagenicity and genotoxicity of sorbic acid-amine reaction products. *Toxicol In Vitro*. 2000;14(5):423-8. doi:10.1016/s0887-2333(00)00035-7.
17. Perez-Prior MT, Manso JA, del Pilasr Carcia-Santos M, Calle E, Casado J. Alkylating potential of potassium sorbate. *J Agric Food Chem*. 2005;53(26):10244-7. doi:10.1021/jf052152p.
18. Muller S, Sanders DA, Antonio MD, Matsis S, Riou JF, Rodriguez R, Balasubramanian S. Pyridostatin analogues promote telomere dysfunction and long-term growth inhibition in human cancer cells. *Org Biomol Chem*. 2012;10(32):6537-46. doi:10.1039/c2ob25830g.
19. Wiecek AJ, Cutty SJ, Kornai D, Parreno-Centteno M, Gourmet LE, Tagliazucchi GM, Jacobson DH, Zhang P, Xiong L, Bond GL, Barr AR, Secrier M. Genomic hallmarks and therapeutic implications of G0 cell cycle arrest in cancer. *Genome Biology*, 2023;24(1):128. doi:10.1186/s13059-023-02963-4.
20. Ichikawa A, Negishi M, Tomita K, Ikegami S. Aphidicolin: A specific inhibitor of DNA synthesis in synchronous mastocytoma P-815 cells. *Jpn J Pharmacol*. 1980; 30(3): 301-8. doi:10.1254/jjp.30.301.
21. Ullah A, Orij R, Brul S, Smits GJ. Quantitative analysis of the modes of growth inhibition by weak acids in *Saccharomyces cerevisiae*. *Appl Environ Microbiol*. 2012;78(23):8377-87. doi:10:1128/AME.02126-12.

22. Zilberstein D, Agmon V, Schuldiner S, Paden E. *Esherichia coli* intracellular pH, membrane potential, and cell growth. *J Bacteriol*. 1984;158(1):246-52 doi:10.1128/jb.158.1.246-252.1984.
23. Stratford M, Anslow PA. Evidence that sorbic acid does not inhibit yeast as a classic weak acid preservative. *Lett Appl Microbiol*. 1998;27(4):203-6. doi: 10.101046/j.1472-765x.1998.00424.x.
24. Bracy D, Holyoak CD, Coote PJ. Comparison of the inhibitory effect of sorbic acid and amphotericin B on *Saccharomyces cerevisiae*: is growth inhibition dependent on reduced intracellular pH?. *Appl Microbiol*. 1998;85(6):1056-66. doi:10.1111/j.1365-2672.1998.tb05271.x.
25. Doyen D, Poet M, Jarretou G, Pisani DF, Tauc M, Cougnon M, Argentina M, Bouret Y, Counillon L. Intracellular pH control by membrane transport in mammalian cells. Insights into the selective advantages of functional redundancy. *Front Mol Biosci*. 2022:9:825028. doi:10.3389/fmolb.2022.825028.
26. Quesada I, Chin WC, Verdugo P. ATP-independent luminal oscillations and release of Ca^{2+} and H^{+} from mast cell secretory granules:implication for signal transduction. *Biophys J*. 2003;85(2):963-70. doi:10.1016/S0006-3495(03)74535-4.
27. Okada Y, Ueyama K, Nishikawa J, semma M, Ichikawa A. Effect of 6-O-α-maltosyl-β cyclodextrin and its cholesterol inclusion complex on cellular cholesterol levels and ABCA1 and ABCG1 expression in mouse mastocytoma P-815 cells. *Carbohydrate Res*. 2012;357:68-74. doi:10.1016/j.carres.2012.04.019.
28. Ishiguro S, Takahashi N, Nemoto K, Negishi M, Ichikawa A. Potentiation of retinoic acid-induced differentiation of HL-60 cells by prostaglandin EP2 receptor. *Prostaglandins Other Lipid Mediat*. 1998;56(2-3):145-53. doi:10.1016/s0090-6980(98)00051-3.
29. Tanaka S, Mikura S, Hashimoto E, Sugimoto Y, Ichikawa A. Ca^{2+} influx-mediated histamine synthesis and IL-6 release in mast cells activated by monomeric IgE. *Eur J Immunol*. 2005;35(2):460-8. doi:10.1002/eji.200425622.
30. Han DW, Lee MH, Kim HH, Hyon SH, Park JC. Epigallocatechin-3-gallate regulates cell growth, cell cycle and phosphorylated nuclear factor-kB in human dermal fibroblast. *Acta Pharmacol Sin*. 2011;32:637-46. doi:10.1038/aps.2011.17.
31. Horiyama S, Honda C, Suwa K, Okada Y, Semma M, Ichikawa A, Takayama M, Negative and positive ion mode LC/MS/MS for sample, selective analysis of sorbic acid. *Chem Pharm Bull*. 2010; 58(1): 106-9. doi:10.1248/cpb.58.106.
32. Thomas JA, Buchsbaum RN, Zimniak A, Racker E. Intracellular pH measurement in Ehrlichascites tumpr cells utilizing spectroscopic probes generated in situ. *Biochemistry*. 1979;18(11): 2210-18. doi:10.1021/bi00578a012.
33. Tanaka S, Takasu Y, Mikura S, Satoh N, Ichikawa A. Antigen-independent induction of histamine synthesis by immunoglobulin E in mouse bone marrow-derived mast cells. *J Exp Med*. 2002;196(2):229-35. doi:10.1084/jem.20012037.
34. Sharom, FJ. The P-glycoprotein efflux pump: how does it transport drugs? *Membrane Biol*. 1997;160:161-75. doi:10.1007/s002329900305.
35. Legend A, Cerrina J, Bonne C, Lockhart A, Benveniste J. Inhibition of rat mast cell degranulation by verapamil. *Agents Actions*. 1984;14(2):153-6. doi:10.1007/BF01966635.
36. Salmond CV, Kroll RG, Booth IR. The effect of food preservatives on the pH homeostasis in *Escherichia coli*. *J Gen Microbiol*. 1984;130:2845-50. doi: 10.1099/00221287-130-11-2845.
37. Schreiber R. Ca^{2+} signaling, intracellular pH and cell volume in cell proliferation. *J Membr Biol*. 2005;205(3):129-37. doi:10.1007/s00232-005-0778-z.
38. Holyak CD, Stratford M, McMulin Z, Cole MB, Klimmins K, Brown, AJ. Coote PJ. Activity of the plasma membrane H^{+}-ATPase and optimal glycolytic flux are required for rapid adaptation and growth of *Saccharomyces cerevisiae* in the presence of the weak-acid preservative sorbic acid. *Appl Environ Microbiol*. 1996;62(9):3158-64. doi:10.1128/aem.62.9.3164.1996
39. Constable PD. Acid-base assessment: when and how to apply Henderson-Hasselbach equation and strong difference theory. *Vet Clin Vet Clin North Am Food Anim Pract*. 2014;30(2):295-316. doi:10.1016/j.cvfa.2014.03.001.
40. Plan TN, Marquis RE. Triclosan inhibition of membrane enzymes and glycolysis of *Streptococcus mutant* in suspensions and biofilms. *Can J Microbiol*. 2006;52(10):977-83. doi:10.1139/w06-055.
41. Alfonso A, Botana, MA, Vieytes MR, Botana LM. Sodium, PMA and calcium play an important role on intracellular pH modulation in rat mast cells. *Cell Physiol Biochem*. 1998;8(6):314-27. doi:101159/000016293.
42. Vilariño N, Vietytes MR, Vieites JM, Botana LM. Role of HCO^{-}_{3} ions in cytosolic pH regulation in rat mast cells: evidence for a new Na^{+}-independent, HCO^{-}_{3}-dependent alkalizing mechanism. *Biochem Biophys Res Commun*. 1998;253(2):320-4. doi:10.1006/bbrc.1998.9615.
43. Alfenso A, Cabado AG, Vieytes MR, Botana LM. Calcium-pH crosstalks in rat mast cells: cytosolic alkalinization, but not intracellular calcium release, is a sufficient signal for degranulation. *Br J Pharmacol*. 2000;130(8):1809-16. doi: 10.1038/si.bip.0703490.
44. Vilariño N, de la Rosa LA, Vieytes MR, Botana LM. The $Cl^{-}HCO_{3}^{-}$ exchanger slows the recovery of acute pHi changes in rat mast cells. *Biochem Pharmacol*. 2003; 65(3):389-96. doi:10.1016/s0006-2952(02)01516-2.
45. Veytia-Bucheli JI, Alvarado-Velázquez DA, Possani LD, González-Amaro R, Rosenstein Y. The Ca^{2+} channel blocker verapamil inhibits the in vitro activation and function of T lymphocytes: A2022 Reappraisal. *Pharmaceutics*. 2022;14(7):1478. doi:10.3390/pharmaceutics 14071478.
46. Simon VR, Moran MF. SERCA activity is required for timely progression through G1/S. *Cell prolif*. 2001;34(1):15-30. doi:10.1046/j.1365-2184.2001.00192.x.
47. Afroze T, Husain M. Cell cycle dependent regulation of intracellar calcium concentration in vascular

smooth muscle cells: a potent target for drug therapy. *Curr Drug Targets Cardiovasc Haematol Disorder*. 2001;1(1):23-40. doi:102174/1568006013338060.

48. Moccia F, Pla AF, Lim D, Lodola F, Gerbino A. Intracellular Ca^{2+} signalling:unexpected new roles for the usual suspect. *Front Physiol*. 2023; 14:1210085. doi:10.3389/fphys.2023.1210085.